

Identification of human cell responses to benzene and benzene metabolites

Bruce Gillis^{a,1}, Igor M. Gavin^{b,c,1}, Zarema Arbieva^c, Stephen T. King^c,
Sundararajan Jayaraman^d, Bellur S. Prabhakar^{b,*}

^a Department of Medicine, University of Illinois, Chicago, IL 60612, USA

^b Department of Microbiology and Immunology, University of Illinois, Chicago, IL 60612, USA

^c Research Resources Center, University of Illinois, Chicago, IL 60612, USA

^d Department of Surgery, College of Medicine, University of Illinois, Chicago, IL 60612, USA

Received 2 February 2007; accepted 8 May 2007

Available online 15 June 2007

Abstract

Benzene is a common air pollutant and confirmed carcinogen, especially in reference to the hematopoietic system. In the present study we analyzed cytokine/chemokine production by, and gene expression induction in, human peripheral blood mononuclear cells upon their exposure to the benzene metabolites catechol, hydroquinone, 1,2,4-benzenetriol, and *p*-benzoquinone. Protein profiling showed that benzene metabolites can stimulate the production of chemokines, the proinflammatory cytokines TNF- α and IL-6, and the Th2 cytokines IL-4 and IL-5. Activated cells showed concurrent suppression of anti-inflammatory cytokine IL-10 expression. We also identified changes in global gene expression patterns in response to benzene metabolite challenges by using high-density oligonucleotide microarrays. Treatment with 1,2,4-benzenetriol resulted in the suppression of genes related to the regulation of protein expression and a concomitant activation of genes that encode heat shock proteins and cytochrome P450 family members. Protein and gene expression profiling identified unique human cellular responses upon exposure to benzene and benzene metabolites.

© 2007 Elsevier Inc. All rights reserved.

Keywords: Benzene; Hydroquinone; 1,4-Benzoquinone; 1,2,4-Benzenetriol; Catechol; Cytokines; Chemokines; Gene expression profiling; Immune response

Benzene is a widely used industrial chemical and one of the most common air pollutants, with emissions reaching 7 million pounds annually in the United States [1]. The role of benzene in the causation of human health effects has long been well established and this is especially so regarding its carcinogenic properties. It is a contaminant that is a by-product of petrochemical processes, vehicular engine exhaust, and cigarette smoking, among other sources. It was among the first confirmed carcinogens established by the International Agency for Research on Cancer [2]. The roles of benzene and benzene metabolites in human health have centered around toxic and injurious effects to the hematopoietic system, including but not limited to bone marrow suppression, particularly in reference to acute and chronic leukemias (reviewed in [3]). Other associa-

tions have been acknowledged, including in regard to lymphomas, myelodysplastic syndrome, multiple myeloma, and malignant melanoma [2].

It is generally agreed that the toxicity of inhaled benzene results from its biotransformation to reactive species. Benzene is metabolized in the liver by cytochrome P4502E1 (CYP2E1) to phenol, which undergoes subsequent hydroxylations to hydroquinone, catechol, and 1,2,4-benzenetriol [4]. Catechol is further oxidized to 1,4-benzoquinone by bone marrow peroxidases or by autoxidation. The intermediate benzene epoxide can also undergo ring opening to *trans*-muconic acid. Because many reactive metabolites are formed during benzene metabolism, it is likely that benzene toxicity is mediated through multiple pathways.

Benzene-induced leukemia is unique because benzene and its metabolites do not have the same DNA-binding properties as “classic carcinogens” [5]. Different mechanisms for benzene-induced toxicity leading to neoplasia have been proposed [6].

* Corresponding author. Fax: +1 312 996 6415.

E-mail address: Bprabhak@uic.edu (B.S. Prabhakar).

¹ These authors contributed equally to this work.

Quinone forms of benzene metabolites can covalently bind to proteins in vitro and act on tubulin, topoisomerase II, and other DNA-associated proteins, eventually leading to leukemia [3,4].

The increased susceptibility to infection as a result of suppression of leukopoiesis is of major significance and may well be the leading cause of death related to chronic exposure to benzene. Benzene exposure leads to a decrease in circulating B and T lymphocytes in vivo [7–10] and inhibition of mitogen-stimulated lymphocyte proliferation [11–13]. No consensus exists on the effects of benzene metabolites on leukocytes. Studies in experimental animals have reported activation of bone marrow macrophages by benzene [14–16] and inhibition of peritoneal macrophage function by benzene metabolites [17–19]. A better mechanistic understanding of how benzene exposure affects the function of the cells of the human immune system might provide a basis for improving treatment of clinical conditions arising from benzene exposure. Consequently, a methodology to track and identify the injurious effects of benzene and benzene metabolites is not only desirable, it is critical to identify appropriate preventive and therapeutic methodologies. Therefore, in this study, an analysis of the effects of benzene and benzene metabolites on human peripheral blood mononuclear cells (PBMC) obtained from both genders and disparate ethnicities, including Caucasians, Asians, African-Americans, and Hispanics, was carried out.

Advances in high-throughput gene microarray technology have made it possible to simultaneously monitor the expression of tens of thousands of genes and to provide a global view of the changes in gene expression in response to exposures to environmental hazards. Analysis of such changes may identify cellular processes and pathways affected by the exposure and provide more comprehensive information on the potential mechanisms of benzene toxicity [20]. For example, by applying microarrays a recent study identified a set of genes differentially expressed in PBMC of benzene-exposed workers [21]. These genes show persistent changes in basal expression presumably due to

chronic benzene exposure. However, identification of early cell responses to acute benzene exposure necessitates gene expression profiling in cells exposed to low levels of benzene/benzene metabolites. By detecting early changes in gene expression one can also identify the “molecular signature” of acute benzene poisoning. To understand the mechanisms of benzene cytotoxicity, we performed a protein and gene expression profiling in PBMC exposed to subtoxic doses of benzene metabolites using DNA and protein microarrays.

Results and discussion

Benzene metabolites can stimulate chemokine/cytokine production by PBMC

Cytokines are important soluble mediators produced in tissues undergoing defense, growth, differentiation, and repair processes [25]. Infection and inflammation result in the induction of cytokines and chemokines mediating immune responses. To investigate the effects of exposures to benzene metabolites on the immune system we measured the secretion of extracellular cytokines by human peripheral blood mononuclear cells exposed to benzene metabolites. Mononuclear cells were isolated from eight healthy donors, males and females representing four ethnic groups, Caucasian, African-American, Hispanic, and Asian, and were challenged with four benzene metabolites, catechol, hydroquinone, 1,2,4-benzenetriol, and 1,4-benzoquinone, at various concentrations. Simultaneous measurement of 15 cytokines and chemokines in the media was performed by using multiplex bead arrays. Cell survival was monitored by propidium iodide staining (not shown). Table 1 shows the concentrations of individual cytokines and chemokines secreted by PBMC in response to benzene metabolite challenges. In contrast to most cytokines, the levels of which remained below the detection limit, significant dose-dependent increases in the expression of most extracellular chemokines

Table 1
Production of cytokines and chemokines by PBMC cultured in the presence of benzene metabolites

	Plasma	Media	Catechol (5 μ M)	Catechol (25 μ M)	Hydroquinone (5 μ M)	Hydroquinone (25 μ M)	Benzenetriol (5 μ M)	Benzenetriol (25 μ M)	Benzoquinone (1 μ M)
GM-CSF	132 \pm 15	<20	<20	<20	<20	<20	<20	<20	<20
IFN- γ	20.2 \pm 1.2	<10	<10	<10	<10	<10	<10	<10	<10
IL-1 β	<100	<50	<50	<50	<50	<50	<50	<50	<50
IL-2	<10	<5	<5	<5	<5	<5	<5	<5	<5
IL-4	81.5 \pm 4.1	<10	<10	<10	<10	<10	<10	<10	<10
IL-5	<5	<3	<3	<3	<3	<3	<3	<3	<3
IL-6	11.2 \pm 0.6	<5	<5	<5	<5	<5	<5	9.1 \pm 1.1	22.7 \pm 1.8
IL-8	17.7 \pm 1.1	144 \pm 28	341 \pm 249	387 \pm 133	416 \pm 21	696 \pm 35	96.2 \pm 4.8	494 \pm 36	820 \pm 161
IL-10	21.7 \pm 1.8	<10	<10	<10	<10	<10	<10	<10	<10
TNF- α	<20	<20	<20	<20	<20	<20	<20	<20	<20
MIP-1 β	79.0 \pm 3.9	41.6 \pm 3.0	<50	<50	<50	<50	<50	60.7 \pm 3	72.9 \pm 7.8
MCP-1	173.2 \pm 9.6	80.8 \pm 30.6	115.4 \pm 45.5	119 \pm 28	101 \pm 18	180 \pm 9	61.4 \pm 3.2	370 \pm 16	227 \pm 61
Eotaxin	143.6 \pm 7.2	6.8 \pm 0.3	9.6 \pm 0.8	10.7 \pm 0.7	8.5 \pm 0.8	15.7 \pm 1.0	6.2 \pm 0.9	20.3 \pm 1.0	18.6 \pm 1.2
MIP-1 α	160.5 \pm 7.6	38.4 \pm 1.9	48.9 \pm 6.4	43.4 \pm 4.1	42.4 \pm 2.1	53.8 \pm 2.7	32.9 \pm 1.6	59.2 \pm 3.0	66.1 \pm 2.1
RANTES	13,087 \pm 654	383 \pm 19	584 \pm 56	622 \pm 36	482 \pm 18	996 \pm 50	386 \pm 64	1174 \pm 51	1286 \pm 207

Concentrations of chemokines and cytokines (pg/ml) in the plasma as well as in conditioned media obtained from PBMC cultures containing the indicated benzene metabolites are shown. “Media” corresponds to the concentration of proteins in unstimulated PBMC cultures. The values indicating the concentrations of various cytokines represent the means \pm SD of results obtained from at least three experiments.

(e.g., IL-8, Eotaxin, MIP1- α , and RANTES) were observed for all benzene metabolite treatments. An increase in MCP-1 chemokine secretion was observed for cells treated with hydroquinone, benzenetriol, and benzoquinone, but not catechol. Treatments with 25 μ M benzenetriol and 1 μ M benzoquinone had the largest effects on the induction of extracellular chemokines. In addition, these treatments resulted in the induction of the inflammatory cytokine IL-6. The observed stimulation of chemokine production by PBMC correlates well with earlier reports of increased IL-8 production by various types of cells in the presence of benzene metabolites [26,27].

Effects of benzene metabolites on mitogen-activated cells

Earlier studies have shown that the effects of benzene metabolites on the functions of the cells of the immune system can vary and depend on the cell type and the stimulus used to induce the immune response. For example, treatment with benzene and its metabolites augmented activation of bone marrow leukocytes by LPS, IFN- γ , and phorbol ester, resulting in an increased production of TNF- α , nitric oxide, and hydrogen peroxide [14,15,28]. In contrast, many studies reported inhibition of the functions of activated leukocytes, including proliferation, phagocytosis, priming for cytolysis, release of hydrogen peroxide, and production of cytokines ([3] and references therein).

To further understand how benzene exposure affects leukocyte function, we examined the effects of benzene metabolites on cytokine production by mitogen-activated leukocytes. PBMC activation by phorbol 12-myristate 13-acetate (PMA) in combination with ionomycin, agents that nonspecifically stimulate PBMC, causes an increase in the production of most cytokines and chemokines [29–31]. Therefore, PBMC were activated by a PMA–ionomycin mixture in the presence of

benzene metabolites and the cytokine production was measured. As shown in Table 2, PBMC stimulation with the PMA–ionomycin mixture induced production of cytokines at 10- to several thousandfold higher levels, resulting in a dramatic increase in cytokine levels in the medium. The effects of benzene metabolites on the secretion of soluble cytokines by activated PBMC varied. For example, dramatic dose-dependent decreases in the production of the chemokines IL-8 and MCP-1 were observed for hydroquinone and catechol, but not for benzenetriol and benzoquinone. Concentrations of other chemokines either slightly increased (e.g., MIP-1 α at 5 μ M benzenetriol and RANTES at 25 μ M catechol and 5 μ M hydroquinone) or remained unchanged. Benzene metabolite treatment also increased secretion of Th2-type cytokines IL-4 and IL-5. All four benzene metabolites augmented production of IL-4, while increased expression of IL-5 was observed only for 5 μ M catechol and 25 μ M hydroquinone treatments. Our observation that benzene metabolites stimulate IL-4 production by activated PBMC correlates well with an earlier report that hydroquinone enhanced IL-4 production by KLH-stimulated CD4⁺ T lymphocytes [32]. Recent studies also suggest that hydroquinone promotes the Th2 type of immune response in LPS-activated macrophages [32,33]. Enhanced production of Th2 cytokines is closely associated with enhanced antibody as well as allergic responses, including the development of asthma.

The effects of benzene metabolites on the expression of proinflammatory cytokines also varied. Stimulation of production of some inflammatory cytokines and the inhibition of others were observed in response to treatment. A dose-dependent increase in the production of TNF- α was observed for all benzene metabolites. Also, IL-6 concentration was increased by treatment with 5 μ M catechol, 25 μ M benzenetriol, and 1 μ M benzoquinone, while IFN- γ production was increased by 25 μ M hydroquinone treatment only. The observed increases

Table 2
Chemokine/cytokine production by PBMC stimulated with PMA and ionomycin in the presence of benzene metabolites

	Unstimulated	PMA + ionomycin							
		Stimulated	Catechol (5 μ M)	Catechol (25 μ M)	Hydroquinone (5 μ M)	Hydroquinone (25 μ M)	Benzenetriol (5 μ M)	Benzenetriol (25 μ M)	Benzoquinone (1 μ M)
GM-CSF	<20	1,224 \pm 94	1,332 \pm 161	980 \pm 180	1,026 \pm 75	980 \pm 180	1,101 \pm 71	1,070 \pm 120	1,249 \pm 62
IFN- γ	<10	4,450 \pm 300	4,158 \pm 584	4,980 \pm 340	5,160 \pm 630	7,600 \pm 1230	5,170 \pm 500	4,430 \pm 240	4,250 \pm 500
IL-1 β	<50	277 \pm 14	258 \pm 13	233 \pm 20	230 \pm 12	236 \pm 12	289 \pm 14	279 \pm 14	292 \pm 15
IL-2	<5	22,870 \pm 1140	20,020 \pm 1830	25,240 \pm 4340	20,890 \pm 1040	22,690 \pm 3370	24,010 \pm 1200	22,110 \pm 1720	18,490 \pm 920
IL-4	<10	98.7 \pm 5.0	129.4 \pm 7.7	125 \pm 11	127.9 \pm 6.4	132.9 \pm 10.4	108.7 \pm 5.4	123.9 \pm 8.9	138.0 \pm 6.9
IL-5	<3	111 \pm 10	137.2 \pm 6.4	1,06.7 \pm 7.6	108.6 \pm 5.4	144 \pm 12	129.9 \pm 7.3	130.9 \pm 9.8	132 \pm 7
IL-6	4.3 \pm 0.2	990 \pm 100	1,301 \pm 65	1,135 \pm 150	1,022 \pm 56	970 \pm 190	1,091 \pm 64	1,210 \pm 110	1,174 \pm 67
IL-8	144 \pm 28	7,260 \pm 540	6,935 \pm 1056	2,810 \pm 440	8,040 \pm 400	4,140 \pm 320	7,370 \pm 370	8,050 \pm 400	8,060 \pm 890
IL-10	<10	410 \pm 20	404 \pm 58	360 \pm 28	365 \pm 28	268 \pm 18	513 \pm 25	324 \pm 36	436 \pm 42
TNF- α	<20	12,890 \pm 440	16,370 \pm 2010	18,940 \pm 6380	13,270 \pm 450	17,700 \pm 5810	14,340 \pm 720	17,140 \pm 690	15,600 \pm 1460
MIP-1 β	41.6 \pm 3.0	14,580 \pm 1970	14,870 \pm 1840	17,220 \pm 2180	18,440 \pm 2160	18,380 \pm 2960	16,670 \pm 750	16,970 \pm 2840	16,010 \pm 1840
MCP-1	80.8 \pm 30.6	612 \pm 27	303 \pm 83	75.6 \pm 10.8	524 \pm 22	113 \pm 15	635 \pm 32	549 \pm 59	587 \pm 26
Eotaxin	6.8 \pm 0.3	47.7 \pm 2.4	47.3 \pm 2.3	47.8 \pm 5.7	52.8 \pm 2.7	48.3 \pm 2.4	52.0 \pm 4.3	48.5 \pm 2.1	47.6 \pm 4.6
MIP-1 α	38.4 \pm 1.9	6,840 \pm 340	7,035 \pm 352	8,450 \pm 1590	7,190 \pm 480	7,600 \pm 820	7,640 \pm 380	7,300 \pm 390	6,240 \pm 250
RANTES	383 \pm 19	9,590 \pm 480	11,310 \pm 1300	11,940 \pm 920	11,450 \pm 570	12,410 \pm 2690	11,690 \pm 1180	11,460 \pm 1410	10,460 \pm 520

PBMC were stimulated with PMA and ionomycin and cultured in the presence of benzene metabolites as described under Materials and methods. “Unstimulated” corresponds to concentration of proteins in the absence of PMA+ ionomycin or any of the metabolites. The values indicating the concentrations of various cytokines represent the means \pm SD of results obtained from at least three experiments.

in TNF- α production by activated PBMC in response to benzene metabolites are in agreement with an earlier report, which showed that benzene treatment can augment TNF- α secretion by LPS-stimulated bone marrow leukocytes [15]. In contrast, secretion of IL-1 β and GM-SCF was suppressed at 25 μ M hydroquinone and catechol, which were consistent with an earlier report of suppression of inflammatory cytokine production by PMA and anti-CD3-stimulated PBMC by hydroquinone and catechol [34]. IL-2 production was decreased at 1 μ M benzoquinone and is consistent with an earlier report on the suppression of mitogen-stimulated IL-2 production by benzoquinone at concentrations that had little to no effect on lymphocyte/macrophage agglutination and blast transformation of human PBMC [35]. We also noted strong inhibition of the production of the anti-inflammatory cytokine IL-10 (Table 2) by higher concentrations of hydroquinone and catechol. Enhanced production of proinflammatory cytokines coupled with the suppression of anti-inflammatory cytokines could lead to tissue damage and predispose an individual to the development of autoimmunity.

Gene expression profiling in 1,2,4-benzenetriol-treated cells

Measurement of cytokine production by PBMC cannot differentiate between the preformed and the de novo synthesized proteins as a consequence of a given treatment. However, high-throughput microarray analysis makes it possible to measure the expression of tens of thousands genes simultaneously. Therefore, we determined the global changes in gene expression following benzene/benzene metabolite treatment. Gene expression analysis was performed by using Affymetrix GeneChip U133A arrays that contained over 22,000 probe sets representing 18,400 transcripts derived from approximately 14,500 well-characterized human genes. Genes that are up or down-regulated in either freshly isolated or cultured PBMC from patients compared to those of healthy individuals were identified using Affymetrix CGOS v1.1 software.

Benzene is hydroxylated by at least two types of cytochrome P450 in liver microsomes [36–38]. Successive hydroxylation steps lead to formation of 1,2,4-benzenetriol, which has been implicated in several aspects of DNA damage related to benzene, an important step in leukemogenesis [39,40]. Unlike hydroquinone and *p*-benzoquinone, whose effects have been studied in greater detail [3], the mechanism by which 1,2,4-benzenetriol exerts its genotoxic effect remains elusive. One hypothesis that it may generate reactive oxygen species, thereby contributing to benzene genotoxicity, is based on the observation that 1,2,4-benzenetriol mediated DNA strand scission by a Fenton-type mechanism occurs when chelated with copper or iron [41]. To shed further light on the mechanisms of benzenetriol toxicity and to identify genes whose expression is affected by benzenetriol treatment, we performed gene expression profiling in PBMC challenged with 1,2,4-benzenetriol.

It was already demonstrated that 25 μ M benzenetriol strongly affected cytokine production by PBMC (Table 1). In contrast, 5 μ M benzenetriol had little to no effect on cytokine

secretion by PBMC and mitogen-induced immune responses (Tables 1 and 2). Therefore, we challenged PBMC with 5 μ M benzenetriol for gene expression profiling. RNA was isolated from treated and untreated PBMC obtained from eight donors and hybridized to an Affymetrix GeneChip Human Genome U133A 2.0 array. Genes whose expression in PBMC changed in treated samples were identified by the Student *t* test. A total of 48 genes that showed altered expression upon exposure at a false discovery rate (FDR) <0.05 were identified (Table 3). Of those genes, 12 were down-regulated and 36 were up-regulated as a result of benzenetriol treatment. Thus, microarray analysis demonstrated that 1,2,4-benzenetriol alters global gene expression pattern in human cells. These alterations in the gene expression are indicative of the cellular functions affected by exposure to this benzene metabolite. Our findings complement other studies on the effects of benzene exposure on gene expression in experimental animals published previously [42–44] and may reflect the underlying mechanisms of cytotoxicity and leukemogenicity of benzene exposure.

Functional categories of genes affected by 1,2,4-benzenetriol treatment

Collections of individual genes obtained via high-throughput transcriptional profiling provide an overwhelming amount of discrete information that is difficult to interpret. The context of molecular and biological functions affected by the treatment can be suggested by applying additional analytical approaches. One of them involves relying on the grouping of genes based on their functional annotation and then identifying relevant groups enriched at a certain statistical significance for differentially expressed genes. This provides clues as to what processes and biological functions are being perturbed during experimental manipulations and are potential key contributors to the observed changes. To determine what cellular functions are affected by 1,2,4-benzenetriol treatment, we identified functional groups in which differentially expressed genes are overrepresented at FDR <0.05 by using the DAVID (Database for Annotation, Visualization, and Integrated Discovery) Web-accessible program at NIAID/NIH (<http://david.abcc.ncifcrf.gov/home.jsp>). Several functional families of genes were strongly affected by 1,2,4-benzenetriol, including protein metabolism, electron transport, and antigen processing and presentation (Table 4). 1,2,4-Benzenetriol has a suppressive effect on expression of genes encoding proteins related to protein synthesis—ribosomal proteins *RPL5* and *RPL15*—as well as components of the translation initiation complex—*EIF3S6IP* and *EIF3S10*. Expression of mRNA splicing factor *SFRS9* was also suppressed. In contrast, we observed a dramatic increase in the expression of chromatin components and the histones H2A and H2B. Expression of a number of heat shock protein genes, including components of the HSP70/HSP90 chaperone system—*HSPA1A*, *HSPA1B*, and *HSP90AA2*—as well as Hsp40 homolog—*DNAJB1*—were also increased. Both HSP70 and HSP90 are also implicated in antigen presentation by the MHC class I complexes [45,46]. We observed a concomitant

Table 3

Genes whose expression in PBMC was significantly affected by treatment with 1,2,4-benzenetriol relative to untreated cells

Gene	Gene symbol	Fold change	<i>p</i> value
Major histocompatibility complex, class II, DP α 1	<i>HLA-DPA1</i>	-3.36	0.0459
Serpin peptidase inhibitor, clade F (α 2 antiplasmin, pigment epithelium-derived factor), member 1	<i>SERPINF1</i>	-2.68	0.0459
Major histocompatibility complex, class II, DP β 1	<i>HLA-DPB1</i>	-1.77	0.0346
Splicing factor, arginine/serine-rich 9	<i>SFRS9</i>	-1.73	0.0459
Chromosome 11 open reading frame 32	<i>C11orf32</i>	-1.71	0.0459
ADP-ribosylation-like factor 6-interacting protein 5	<i>ARL6IP5</i>	-1.49	0.0200
Ribosomal protein L5	<i>RPL5</i>	-1.46	0.0189
Eukaryotic translation initiation factor 3, subunit 6-interacting protein	<i>EIF3S6IP</i>	-1.45	0.0500
Eukaryotic translation initiation factor 3, subunit 10 θ , 150/170 kDa	<i>EIF3S10</i>	-1.44	0.0497
Ribosomal protein L15	<i>RPL15</i>	-1.42	0.0459
Adenylosuccinate lyase	<i>ADSL</i>	-1.34	0.0473
Potassium voltage-gated channel, Shal-related subfamily, member 1	<i>KCND1</i>	-1.28	0.0475
Protein phosphatase 1, regulatory (inhibitor) subunit 12A	<i>PPP1R12A</i>	1.31	0.0378
Kelch-like ECH-associated protein 1	<i>KEAP1</i>	1.34	0.0409
Heat shock protein 90 kDa α (cytosolic), class A member 1	<i>HSP90AA1</i>	1.36	0.0459
NCK adaptor protein 2	<i>NCK2</i>	1.42	0.0305
DnaJ (Hsp40) homolog, subfamily B, member 1	<i>DNAJB1</i>	1.44	0.0459
GA binding protein transcription factor, β subunit 2	<i>GABPB2</i>	1.45	0.0346
ERO1-like (<i>Saccharomyces cerevisiae</i>)	<i>ERO1L</i>	1.45	0.0497
Golgi associated, γ adaptin ear containing, ARF-binding protein 1	<i>GGAI</i>	1.47	0.0383
Ferredoxin reductase	<i>FDXR</i>	1.54	0.0497
ATP citrate lyase	<i>ACLY</i>	1.54	0.0200
SH3-domain-binding protein 2	<i>SH3BP2</i>	1.60	0.0475
Prune homolog (<i>Drosophila melanogaster</i>)	<i>PRUNE</i>	1.60	0.0495
Heat shock 70-kDa protein 1A	<i>HSPA1A</i>	1.62	0.0409
Chromosome 1 open reading frame 78	<i>C1orf78</i>	1.63	0.0346
KIAA0317	<i>KIAA0317</i>	1.65	0.0459
Pleckstrin homology-like domain, family A, member 1	<i>PHLDA1</i>	1.76	0.0200
RAB22A, member RAS oncogene family	<i>RAB22A</i>	1.78	0.0262
ATP-binding cassette, subfamily C (CFTR/MRP), member 1	<i>ABCC1</i>	1.80	0.0200
Thioredoxin reductase 1	<i>TXNRD1</i>	1.83	0.0475
Tumor necrosis factor (TNF superfamily, member 2)	<i>TNF</i>	1.83	0.0459
Cytochrome P450, family 1, subfamily B, polypeptide 1	<i>CYP1B1</i>	1.98	0.0346
Tubulin tyrosine ligase-like family, member 4	<i>TTLA4</i>	2.07	0.0378
BTB and CNC homology 1, basic leucine zipper transcription factor 1	<i>BACH1</i>	2.12	0.0378
Jumonji, AT-rich interactive domain 2	<i>JARID2</i>	2.13	0.0473

Table 3 (continued)

Gene	Gene symbol	Fold change	<i>p</i> value
Guanine nucleotide binding protein (G protein), α Z polypeptide	<i>GNAZ</i>	2.15	0.0459
Cortactin	<i>CTTN</i>	2.22	0.0495
Histone 2, H2aa // similar to histone H2A.o (H2A/o) (H2A.2) (H2a-615) // histone H2A/r	<i>HIST2H2AA3</i>	2.59	0.0475
Adipose differentiation-related protein	<i>ADFP</i>	2.85	0.0182
Cytochrome P450, family 27, subfamily A, polypeptide 1	<i>CYP27A1</i>	3.06	0.0182
Histone 1, H2bg	<i>HIST1H2BG</i>	3.36	0.0409
Ras-induced senescence 1	<i>TMEM158</i>	3.63	0.0206
Integrin, β 3 (platelet glycoprotein IIIa, antigen CD61)	<i>ITGB3</i>	3.67	0.0495
Heat shock 70-kDa protein 1B	<i>HSPA1B</i>	4.88	0.0176
Hairy and enhancer of split 1 (<i>D. melanogaster</i>)	<i>HES1</i>	5.57	0.0346
Integrin- α 2b (platelet glycoprotein IIb of IIb/IIIa complex, antigen CD41)	<i>ITGA2B</i>	6.01	0.0330
Glycoprotein Ib (platelet), β polypeptide // septin 5	<i>GP1BB</i>	7.71	0.0189

The *p* value is the statistical measure of differential expression of the indicated gene relative to unstimulated control cells.

decrease in the expression of genes encoding components of MHC class II complexes—*HLA-DPA1* and *HLA-DPB1*. 1,2,4-Benzenetriol also induced expression of the cytochrome P450 genes *CYP27A1* and *CYP1B1*, which correlates well with the role of these P450 cytochromes in the metabolism of aromatic hydrocarbons [47,48]. Induction of other members of

Table 4

Functional groups overrepresented among differentially expressed genes

Functional group	<i>p</i> value	Gene symbols
Protein metabolism	7.1×10^{-2}	<i>SFRS9</i> , <i>EIF3S6IP</i> , <i>EIF3S10</i> , <i>RPL15</i> , <i>RPL5</i> , <i>HIST2H2AA3</i> , <i>HIST1H2BG</i> , <i>DNAJB1</i> , <i>HSP90AA1</i> , <i>HSPA1A</i> , <i>HSPA1B</i> , <i>GGAI</i> , <i>ERO1L</i> , <i>KIAA0317</i> , <i>ABCC1</i> , <i>TTLA4</i> , <i>NCK2</i>
Endoplasmic reticulum	2.7×10^{-2}	<i>ARL6IP5</i> , <i>ERO1L</i> , <i>HSPA1A</i> , <i>CYP1B1</i> , <i>GNAZ</i> , <i>ADFP</i> , <i>HSPA1B</i>
Generation of precursor metabolites and energy	5.8×10^{-2}	<i>FDXR</i> , <i>ERO1L</i> , <i>ACLY</i> , <i>CYP27A1</i> , <i>TXNRD1</i> , <i>CYP1B1</i>
Electron transport	4.3×10^{-2}	<i>FDXR</i> , <i>ERO1L</i> , <i>CYP27A1</i> , <i>TXNRD1</i> , <i>CYP1B1</i>
Antigen processing and presentation	9.0×10^{-3}	<i>HSP90AA1</i> , <i>HSPA1A</i> , <i>HSPA1B</i> , <i>HLA-DPB1</i> , <i>HLA-DPA1</i>
Hematopoietic cell lineage	1.1×10^{-2}	<i>TNF</i> , <i>GP1BB</i> , <i>ITGB3</i> , <i>ITGA2B</i>
Response to protein stimulus	1.8×10^{-2}	<i>DNAJB1</i> , <i>HSP90AA1</i> , <i>HSPA1A</i> , <i>HSPA1B</i>
ECM-receptor interaction	9.2×10^{-2}	<i>GP1BB</i> , <i>ITGB3</i> , <i>ITGA2B</i>

The *p* value is the statistical measure of overrepresentation of a corresponding functional group among differentially expressed genes.

the cytochrome P450 family, e.g., cytochrome P450 2E1 (*CYP2E1*), by benzene was observed earlier [37,38].

Molecular interaction networks activated in response to 1,2,4-benzenetriol treatment

To reconstitute a system of molecular responses initiated as a consequence of exposure to benzene/benzene derivatives, we studied networks of protein interactions that engaged the differentially expressed genes which were identified in our study. All 48 significantly differentially expressed genes were analyzed against a database of known molecular pathways (ResNet, Ariadne Genomics, Inc.) and the results of these analyses are depicted in Fig. 1. No direct responders to benzene treatment among differentially expressed genes were identified; however, a few of them interact directly with “primary responders” to the treatment (*CYP2E1*, *IL2*, *CSF1*, *CSF2*, *CSF3*, and *TP53*), thus facilitating a cascade of subsequent reactions. Each of them is involved in one of the following types of interactions with differentially expressed genes: regulation, direct regulation, expression, or binding. Details of these interactions and supporting facts are given in Table A of the supplementary material. A list of participating differentially expressed genes is given in Table B of the supplementary material. One of the central genes in the scheme is the tumor necrosis factor (TNF) gene, the expression of which in

benzenetriol-treated cells increased 1.8-fold. TNF regulates many downstream genes whose expression changed in benzenetriol-treated cells and, as shown previously, may also engage the p53-mediated apoptotic pathway [49]. It has been shown that benzene exposure in mice activates p53-regulated cell cycle genes and apoptotic genes, suggesting a role for p53 protein in benzene-induced G2/M arrest and apoptosis [43,50]. Consistent with these studies, the *TP53* gene did not appear on our list of differentially expressed genes; however, p53 regulates many downstream genes affected by benzenetriol treatment (Fig. 1).

Validation of gene expression array data by real-time PCR

To confirm the results of gene profiling independently and validate the potential targets for detecting benzene exposure, we performed a quantitative real-time PCR analysis of the expression of a number of differentially expressed genes identified in the gene array screen. Five target sequences representing three positively regulated genes, *CYP1B1*, *CYP27A1*, and *TNF*, as well as two of the most strongly down-regulated genes, *HLA-DPA1* and *SERPINF1* were analyzed. The importance of cytochrome P450 family proteins in the metabolism of aromatic hydrocarbons was demonstrated earlier [47,48]. TNF plays a central role in the molecular interaction network activated by benzene exposure (Fig. 1). Real-time PCR was performed on

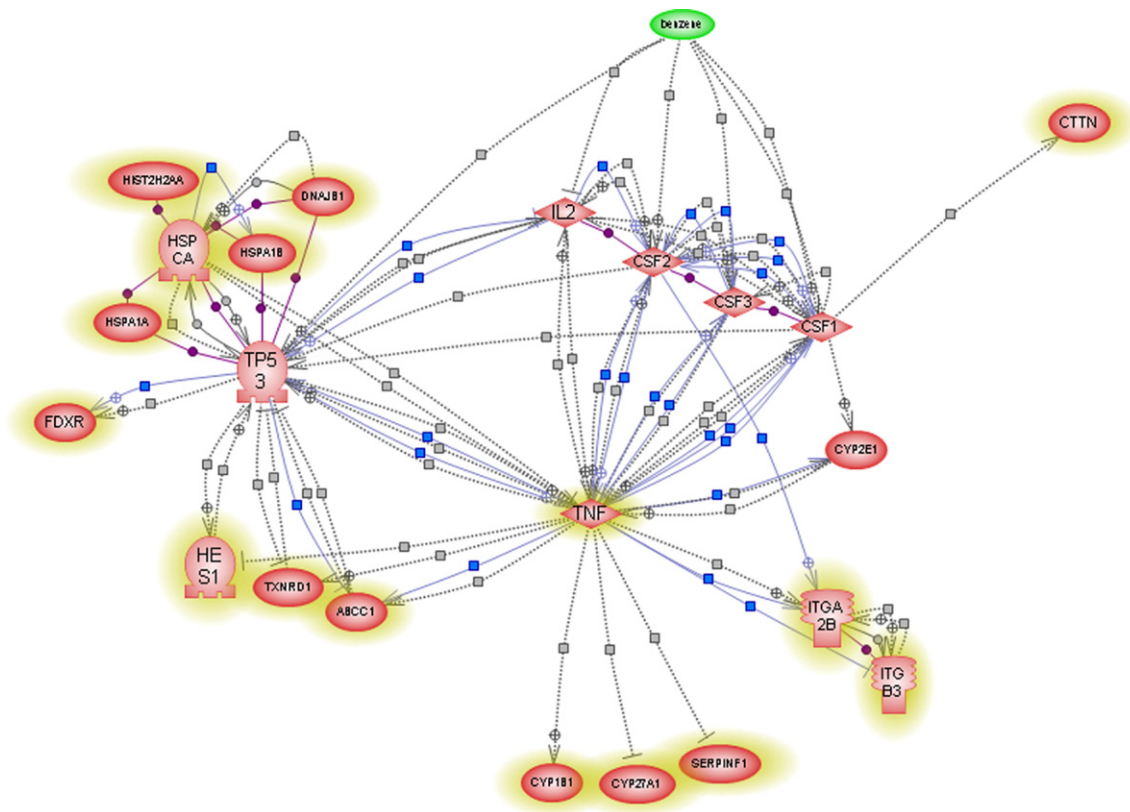


Fig. 1. A network of molecular interactions between proteins engaged in response to benzene treatment. Nodes represent proteins (in red) and small molecules (in green). Nodes highlighted in yellow are differentially expressed in our system. Lines depict different types of interactions/regulations between the nodes: expression (in blue), regulation (marked by gray squares), direct regulation (marked by gray circles), and binding (in purple).

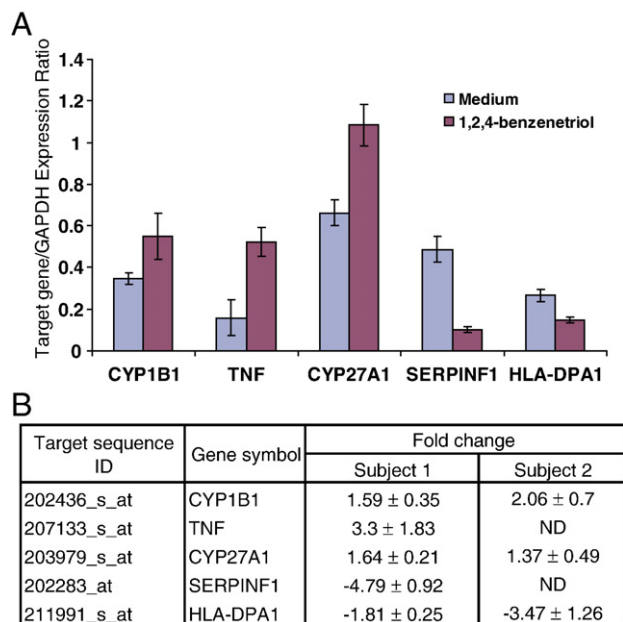


Fig. 2. Quantitative real-time PCR analysis of gene expression in 1,2,4-benzenetriol-treated PBMC. Real-time RT-PCR was performed on total RNA from PBMC cultured either in the presence (1,2,4-benzenetriol) or in the absence (Medium) of 5 μ M 1,2,4-benzenetriol as described under Materials and methods. The signal corresponding to each target gene was normalized to the GAPDH signal. (A) Relative expression of five gene targets in PBMC of subject 1. (B) Expression fold change in treated vs untreated PBMC samples of two subjects; a positive value indicates an increase, while a negative value indicates a decrease; ND, not detected.

cDNA samples corresponding to either untreated or 1,2,4-benzenetriol-treated PBMC from two subjects using primers to the target sequences identified on Affymetrix GeneChip U133A. As shown in Fig. 2, the change in the expression of the five target genes upon benzenetriol treatment strongly correlated with the gene expression array data (Table 3). *CYP1B1*, *CYP27A1*, and *TNF* mRNAs were elevated in the 1,2,4-benzenetriol-treated sample, while *HLA-DPA1* and *SERPINF1* mRNAs were suppressed (Fig. 2A). The fold change of the mRNAs was also consistent with the average fold change determined in the gene array analysis (Fig. 2B). Independent measurement of the changes in the expression of these genes by real-time PCR further validates the gene expression data and makes it possible to employ targets identified in this screen for determining benzene exposure.

Identification of individual human cellular responses to chemicals has long been desired because it allows for a comprehensive determination of fundamental human health responses to such compounds. In the past, we have primarily depended upon epidemiologic analyses to uncover suspected and potential injurious effects of chemical agents. Now, by being able to rely upon gene expression analyses, we are able to directly define the specific impact of a given toxic substance and its metabolites has on human cells. In this study, we have utilized such an approach to comprehensively assess the unique human cellular responses to exposures to benzene and its metabolites. To eliminate potential biases resulting from gender

and ethnicity, we used blood taken from both genders and four major ethnic/racial variants.

The information presented in this study not only offers clarity for determining injurious chemical exposures, but it also provides a methodology for eliminating inaccurate diagnoses and erroneous conclusions following such an exposure. It is no longer sufficient to state that a compound such as benzene is or is not potentially harmful. It is necessary to determine whether there indeed have been injurious exposures that have resultant and quantifiable human health effects. Until recently, it has been very difficult if not impossible to make such a determination. The global gene expression patterns that we have elucidated clearly document the specific cellular impact of benzene and benzene metabolites. Moreover, our study shows that this methodology as well as protein profiling can be used to detect the human health effects of other environmental toxicants, including chemical substances. The information that will be obtained through such methodologies offers a starting point for developing human health treatment protocols. And the applicability of this information not only portends consideration of appropriate therapeutics but it also allows for the monitoring of the effectiveness of any treatment at discrete cellular levels.

In summary, gene and protein expression profiling is an elegant technological breakthrough that offers multiple human health applications that are founded on unique DNA-based and protein-based cellular patterns. Such individual cellular response patterns obtained from across genders and ethnicities as have been identified regarding benzene and benzene metabolites indicate a reliable approach for understanding whether chemical agents and their metabolites are toxic and/or injurious. The applications that will evolve from this information will translate into more accurate human health diagnoses and more appropriate therapies.

Materials and methods

Isolation of peripheral blood mononuclear cells

Twenty to thirty milliliters of blood was drawn in tubes containing EDTA by venipuncture from Caucasian, African American, Hispanic, and Asian male and female healthy volunteers after obtaining appropriate consent. This study was approved by the Institutional Review Board of the University of Illinois at Chicago. Blood was diluted 1:1 in Hanks' balanced salt solution (HBSS; Invitrogen, Carlsbad, CA, USA) and layered on top of Ficoll (Histopaque; Sigma, St. Louis, MO, USA). After 20 min of centrifugation at room temperature at 1200 rpm, the interphase containing PBMC was harvested. After the cells were washed in HBSS, viability was determined using trypan blue exclusion. Cells were divided equally into two portions. One portion was used immediately for assays and the other was cultured.

In vitro culture of PBMC

Cells were adjusted to 1×10^6 cells/ml using complete RPMI medium supplemented with antibiotics and 10% fetal bovine serum. Cells (1×10^6) were placed in a 24-well tissue culture plate. Triplicate wells were stimulated with 1 μ g/ml PMA (Sigma) and 1 μ g/ml ionomycin (EMD Biosciences, Darmstadt, Germany), agents that nonspecifically stimulate PBMC. Cells cultured in the medium served as controls for basal levels of cytokines/chemokines. Cells were also cultured in the presence of different benzene metabolites used at various concentrations.

Collection of plasma and culture supernatants for cytokine/chemokine multiplex assays

As soon as the blood was collected, a 2-ml aliquot was centrifuged at 2000 rpm for 5 min to obtain plasma. This was centrifuged at 15,000 g and immediately placed at and -80°C for storage. After overnight culture of PBMC either in the medium alone or in the presence of various stimulating agents, the supernatants were removed and centrifuged and the clear cell-free culture media were collected and placed at and -80°C until used in various assays.

Collection of cells for RNA isolation

Freshly isolated and cultured PBMC were collected by centrifugation at 2000 rpm for 5 min. Cells were washed with PBS and RNA was isolated using Trizol reagent (Invitrogen). Five hundred microliters of Trizol was added to the tube and cells were lysed by passing the solution through a micropipette tip. One hundred microliters of chloroform was added to the samples, which were then vortexed for 15 s. The samples were centrifuged at 15,000 g for 10 min and the aqueous phase was collected. RNA was precipitated from the aqueous phase by adding 250 μl of isopropanol followed by centrifugation at 15,000 g for 10 min. The RNA pellets were washed with 500 μl of 70% ethanol, dried, and dissolved in 15 μl of deionized water. RNA concentration was determined by the absorbance at 260 nm and its quality was assessed by agarose gel electrophoresis. RNA samples were stored at -80°C . When necessary, PBMC were immediately placed at -80°C and RNA was isolated at a later time as described above.

Cytokine assay

Cytokine and chemokine concentrations in plasma as well as in culture supernatants were measured by multiplex bead immunoassay using a BioPlex fluorescence bead reader (Bio-Rad, Hercules, CA, USA). Three panels of antibody-conjugated beads for measuring inflammatory cytokines (GM-CSF, IL-1 β , IL-6, IL-8, TNF- α), Th1/Th2 cytokines (IFN- γ , IL-2, IL-4, IL-5, IL-10), and chemokines (MIP-1 α , MIP-1 β , MCP-1, eotaxin, RANTES) (BioSource reagents from Invitrogen) were mixed and the concentrations of individual proteins in supernatants were determined according to the manufacturer's instructions. The levels of cytokine secretion upon PBMC activation were compared to those obtained from unstimulated control cells.

Collection of gene expression data

An oligonucleotide-based Affymetrix Human U133A GeneChip Array was employed for the study. The HG-U133A Array includes representation of the RefSeq database sequences and probe sets related to sequences previously represented on the Human Genome U95Av2 Array. Total cellular RNA was isolated from eight individuals using RNeasy columns (Qiagen, Valencia, CA, USA) according to the manufacturer's protocol. All labeling reactions and hybridizations were carried out according to the standard GeneChip eukaryotic target labeling protocol (Affymetrix, Santa Clara, CA, USA). Briefly, 1–5 μg of total cellular RNA per sample was used to synthesize the double-stranded cDNA, which then was transcribed in vitro in the presence of biotinylated dNTPs (Enzo Diagnostics, Farmingdale, NY, USA). Biotinylated target cRNA was fragmented and brought up in hybridization mix. Successful labeling of all the samples (a minimum of 15 μg of in vitro-transcribed product per sample) was followed by the test array hybridizations. Test hybridizations were performed with "Test3" arrays (Affymetrix) to ensure quality of the biotinylated target. The Test3 array contains probe sets corresponding to commonly expressed genes from the human, mouse, rat, and yeast genomes, along with prokaryotic control genes. Successful test hybridizations indicating efficient cRNA amplification and strong target hybridization activity were followed by actual experimental hybridizations. One GeneChip U133A array was used per RNA sample. Hybridizations were followed by staining and binding to biotin of a streptavidin-conjugated fluorescent marker. Detection of bound probe was achieved following laser excitation of the fluorescent marker and scanning of the resultant emission spectra using a scanning confocal laser microscope (Probe Array Scan, Agilent Technologies). Data acquisition was performed using GCOS (Affymetrix GeneChip Operating Software Package).

Collected hybridization images were subjected to quality control to remove from analysis arrays that failed to meet criteria both suggested by Affymetrix and developed internally. These quality requirements include low Q-noise (1–10), low background (less than 100), sample-dependent percentages of probes detected as present (20–50% for mammals), 3'/5' ratios of no more than 3, hybridization efficiency defined by intensities detected for the spike control probe sets (preferably higher than 2000 fluorescence units), and minimal deviation of scaling factors for the whole set of arrays to be analyzed.

Gene expression data analysis

Data normalization, background correction, and all subsequent statistical tests for significant differential expression were performed with the use of the S+ Array Analyzer statistical software package (Insightful). CEL files were exported from GCOS into the Array Analyzer module of the package and used for calculation of the Affymetrix expression summary (RMA method, quantiles normalization). Student's *t* test was applied to calculate statistically significant differentially expressed genes, and raw *p* values were corrected for FDR using the Benjamini and Hochberg procedure [22]. Only genes with FDR < 0.05 were used for further analysis.

Differentially expressed transcripts were initially annotated with the use of the NetAffx Analysis Center (<http://www.affymetrix.com>) according to the most up-to-date version of the Gene Ontology Database (<http://www.geneontology.org/>). Further biological annotation was performed with the DAVID Web-based functional annotation tool (<http://david.abcc.ncifcrf.gov>) and the PathwayStudio functional annotation software package (Ariadne Genomics).

Real-time PCR

Forward and reverse primers were synthesized to the target sequences represented by the corresponding probes on the Affymetrix GeneChip U133A arrays. The target sequence IDs are listed in Fig. 2. All primers were designed using the PrimerQuest software (Integrated DNA Technologies, Coralville, IA, USA). The primer sequences were as follows: *TNF*-forward, TGATCCCTGACATCTGGAATCTGG, reverse, TGGAAACATCTGGAGAGAGGAAGG; *CYP11B1* forward, TATGTCAACCAGGTCCAGATGTGC, reverse, TAAGC-CAGGTAACTCCAAGCACC; *HLA-DPA1* forward, CCAAGAGCCAATC-CAGATGCCTG, reverse, AGGACGGTGCCACGATGATG; *SERPINF1* forward, GCATGAGTATCATCTTCTCTCTGCCC, reverse, ACGGTCTT-CAGTTCTCGGTCTATG; *CYP27A1* forward, ATGTCTCAGATGAGGAGG-GAGAGAAG, reverse, TTTAGCTGAGAGGGAGTTGCTC. *GAPDH* primers were described earlier [23].

cDNA was synthesized from total RNA isolated from PBMC cultured either in the absence or in the presence of 5 μM 1,2,4-benzenetriol by using the First Strand cDNA Synthesis Kit (Fermentas, Hanover, MD, USA) with oligo(dT) primers, according to the manufacturer's protocol. Briefly, 200 ng of total RNA was used as a template in a 20- μl cDNA synthesis. One microliter of oligo (dT)₁₈ primer and 4 μl of 5 \times reaction buffer were added to the sample and the reaction volume was adjusted to 15 μl with DEPC water. The samples were heated to 60 $^{\circ}\text{C}$ for 5 min to denature the template. The samples were subsequently placed on ice and 1 μl of RNase inhibitor, 2 μl of 10 mM dNTP mix, and 2 μl of reverse transcriptase (20 U/ μl) were added. The samples were then incubated at 37 $^{\circ}\text{C}$ for 60 min. The reaction was stopped by heating the samples at 70 $^{\circ}\text{C}$ for 10 min and stored at -70°C . Negative control reactions were made from total RNA for each sample and then put through reverse transcription in which all reagents except RT were present. This was used as an RT control in the real-time PCR to confirm that no genomic DNA was present in the total RNA samples.

Primer sets were first validated by a conventional PCR. The primers were tested in 25- μl reactions containing 1 μM forward and reverse primer, 1 μl of control cDNA template, 3 mM MgCl₂, 1 \times PCR buffer, and 0.7 unit of AmpliTaq Gold (Applied Biosystems, Foster City, CA, USA). The samples were initially denatured at 95 $^{\circ}\text{C}$ for 5 min and then were subjected to 30 cycles of PCR with denaturation at 95 $^{\circ}\text{C}$ for 30 s and annealing/extension at 60 $^{\circ}\text{C}$ for 1 min. PCR product size was validated by gel electrophoresis in a 3% NuSieve agarose (FMC, Rockland, ME, USA) TAE gel stained with ethidium bromide.

A real-time quantitative PCR assay was carried out using an ABI 7900HT detection system and the SYBR Green PCR Mix for ABI Prism (Applied Biosystems). Samples were measured in triplicate. In short, 12.5 μ l Master Mix containing Taq DNA polymerase, reaction buffer, deoxynucleoside triphosphate mix, and SYBR Green I dye were combined with equal volume of 0.4 μ M appropriate primers and cDNA.

For quantitation purposes, 2 μ l of cDNA was amplified from each group. The thermocycling protocol was 50 °C for 2 min, denaturation at 95 °C for 10 min, and 40 cycles of PCR at 95 °C for 15 s and 60 °C for 60 s. The temperature transition rate was 20 °C/s. Fluorescence was measured at the end of each extension step. After amplification, a melting curve was acquired by heating the product at 20 °C/s to 95 °C, cooling it at 20 °C/s to 60 °C, incubating at 60 °C for 20 s, and then slowly heating it at 0.1 °C/s to 95 °C. Fluorescence was measured through the slow heating phase. Melting curves were used to confirm the specificity of the gene-specific qPCR primers in addition to determining their specificity by gel electrophoresis. To correct for potential variances between samples in mRNA extraction and RT efficacy and for variances in pipetting, the mRNA quantity was normalized to the mRNA quantity of the endogenous control gene *GAPDH* from the same sample. As a negative control, total RNA samples were DNase treated and then put through reverse transcription in which all reagents except for RT were present. The resulting samples did not produce any PCR product, confirming that there was no genomic DNA contamination in the samples tested. The C_T (threshold cycle) values were calculated with the sequence detection system 7900HT (Applied Biosystems). The baseline used was an average of C_T values from PCR cycles 3–12, plus C_T generated at 10 \times the standard deviation. The C_T values were exported to Excel to calculate expression ratios for each gene.

The data were analyzed using the relative standard curve method as previously described [24] and per the ABI standard protocol. Control cDNA was serially diluted and used in the qPCR assay for each primer set. A standard curve was generated for each primer set by a least-squares fit of the log RNA concentration to the C_T . The C_T for each sample and control were converted to RNA quantity via the standard curve constants for each primer set. The expression ratio of the genes of interest was calculated by normalizing the RNA quantities for each primer set to that of *GAPDH*.

Appendix A. Supplementary data

Supplementary data associated with this article can be found, in the online version, at doi:10.1016/j.ygeno.2007.05.003.

References

- [1] D.L. Bayliss, C. Chen, A. Jarabek, B. Sonawane, L. Valcovic, Carcinogenic Effects of Benzene: an Update, U.S. Environmental Protection Agency, Washington, DC, 1998.
- [2] IARC, Benzene, Overall Evaluations of Carcinogenicity: an Updating of Selected IARC Monographs from Volumes 1 to 42, International Agency for Research on Cancer, Lyon, 1987.
- [3] R. Snyder, Benzene and leukemia, *Crit. Rev. Toxicol.* 32 (2002) 155–210.
- [4] R. Snyder, Xenobiotic metabolism and the mechanism(s) of benzene toxicity, *Drug Metab. Rev.* 36 (2004) 531–547.
- [5] M.T. Smith, The mechanism of benzene-induced leukemia: a hypothesis and speculations on the causes of leukemia, *Environ. Health Perspect.* 104 (Suppl. 6) (1996) 1219–1225.
- [6] J. Whysner, M.V. Reddy, P.M. Ross, M. Mohan, E.A. Lax, Genotoxicity of benzene and its metabolites, *Mutat. Res.* 566 (2004) 99–130.
- [7] K. Aoyama, Effects of benzene inhalation on lymphocyte subpopulations and immune response in mice, *Toxicol. Appl. Pharmacol.* 85 (1986) 92–101.
- [8] N. Rothman, G.L. Li, M. Dosemeci, W.E. Bechtold, G.E. Marti, Y.Z. Wang, M. Linet, L.Q. Xi, W. Lu, M.T. Smith, N. Titenko-Holland, L.P. Zhang, W. Blot, S.N. Yin, R.B. Hayes, Hematotoxicity among Chinese workers heavily exposed to benzene, *Am. J. Ind. Med.* 29 (1996) 236–246.
- [9] G.M. Farris, S.N. Robinson, B.A. Wong, V.A. Wong, W.P. Hahn, R. Shah, Effects of benzene on splenic, thymic, and femoral lymphocytes in mice, *Toxicology* 118 (1997) 137–148.
- [10] M.G. Rozen, C.A. Snyder, Protracted exposure of C57BL/6 mice to 300 ppm benzene depresses B- and T-lymphocyte numbers and mitogen responses: evidence for thymic and bone marrow proliferation in response to the exposures, *Toxicology* 37 (1985) 13–26.
- [11] R.W. Pfeifer, R.D. Irons, Effect of benzene metabolites on phytohemagglutinin-stimulated lymphopoiesis in rat bone marrow, *J. Reticuloendothel. Soc.* 31 (1982) 155–170.
- [12] M.G. Rozen, C.A. Snyder, R.E. Albert, Depressions in B- and T-lymphocyte mitogen-induced blastogenesis in mice exposed to low concentrations of benzene, *Toxicol. Lett.* 20 (1984) 343–349.
- [13] R.W. Pfeifer, R.D. Irons, Inhibition of lectin-stimulated lymphocyte agglutination and mitogenesis by hydroquinone: reactivity with intracellular sulfhydryl groups, *Exp. Mol. Pathol.* 35 (1981) 189–198.
- [14] D.L. Laskin, L. MacEachern, R. Snyder, Activation of bone marrow phagocytes following benzene treatment of mice, *Environ. Health Perspect.* 82 (1989) 75–79.
- [15] L. MacEachern, D.L. Laskin, Increased production of tumor necrosis factor- α by bone marrow leukocytes following benzene treatment of mice, *Toxicol. Appl. Pharmacol.* 113 (1992) 260–266.
- [16] L. MacEachern, R. Snyder, D.L. Laskin, Alterations in the morphology and functional activity of bone marrow phagocytes following benzene treatment of mice, *Toxicol. Appl. Pharmacol.* 117 (1992) 147–154.
- [17] M.J. Klan, D.O. Adams, J.G. Lewis, Effects of exposure to benzene in vivo on the murine mononuclear phagocyte system, *Toxicol. Appl. Pharmacol.* 103 (1990) 198–205.
- [18] J.G. Lewis, B. Odom, D.O. Adams, Toxic effects of benzene and benzene metabolites on mononuclear phagocytes, *Toxicol. Appl. Pharmacol.* 92 (1988) 246–254.
- [19] B.W. Manning, D.O. Adams, J.G. Lewis, Effects of benzene metabolites on receptor-mediated phagocytosis and cytoskeletal integrity in mouse peritoneal macrophages, *Toxicol. Appl. Pharmacol.* 126 (1994) 214–223.
- [20] M.T. Smith, R. Vermeulen, G. Li, L. Zhang, Q. Lan, A.E. Hubbard, M.S. Forrest, C. McHale, X. Zhao, L. Gunn, M. Shen, S.M. Rappaport, S. Yin, S. Chanock, N. Rothman, Use of ‘omic’ technologies to study humans exposed to benzene, *Chem. Biol. Interact.* 153–154 (2005) 123–127.
- [21] M.S. Forrest, Q. Lan, A.E. Hubbard, L. Zhang, R. Vermeulen, X. Zhao, G. Li, Y.Y. Wu, M. Shen, S. Yin, S.J. Chanock, N. Rothman, M.T. Smith, Discovery of novel biomarkers by microarray analysis of peripheral blood mononuclear cell gene expression in benzene-exposed workers, *Environ. Health Perspect.* 113 (2005) 801–807.
- [22] Y. Benjamini, Y. Hochberg, Controlling the false discovery rate: a practical and powerful approach to multiple testing, *J. R. Stat. Soc., Ser. B* 57 (1995) 289–300.
- [23] R.V. Gutala, P.H. Reddy, The use of real-time PCR analysis in a gene expression study of Alzheimer’s disease post-mortem brains, *J. Neurosci. Methods* 132 (2004) 101–107.
- [24] M.W. Pfaffl, A new mathematical model for relative quantification in real-time RT-PCR, *Nucleic Acids Res.* 29 (2001) e45.
- [25] S.J. Hopkins, The pathophysiological role of cytokines, *Leg. Med. (Tokyo)* 5 (Suppl. 1) (2003) S45–S57.
- [26] D. Bironaite, D. Siegel, J.L. Moran, B.B. Weksler, D. Ross, Stimulation of endothelial IL-8 (eIL-8) production and apoptosis by phenolic metabolites of benzene in HL-60 cells and human bone marrow endothelial cells, *Chem. Biol. Interact.* 149 (2004) 177–188.
- [27] M. Miyazawa, Y. Ito, Y. Yoshida, H. Sakaguchi, H. Suzuki, Phenotypic alterations and cytokine production in THP-1 cells in response to allergens, *Toxicol. In Vitro* 21 (3) (2007) 428–437.
- [28] J.D. Laskin, N.R. Rao, C.J. Punjabi, D.L. Laskin, R. Snyder, Distinct actions of benzene and its metabolites on nitric oxide production by bone marrow leukocytes, *J. Leukocyte Biol.* 57 (1995) 422–426.
- [29] T. Tsuchida, T. Sakane, Intracellular activation signal requirements for the induction of IL-2 responsiveness in resting T cell subsets in humans, *J. Immunol.* 140 (1988) 3446–3449.
- [30] J.A. Kurtzals, M. Kemp, L.K. Poulsen, M.B. Hansen, A. Kharazmi, T.G. Theander, Interleukin-4 and interferon-gamma production by Leishmania

- stimulated peripheral blood mononuclear cells from nonexposed individuals, *Scand. J. Immunol.* 41 (1995) 343–349.
- [31] J. Jason, J. Larned, Single-cell cytokine profiles in normal humans: comparison of flow cytometric reagents and stimulation protocols, *J. Immunol. Methods* 207 (1997) 13–22.
- [32] M.H. Lee, S.W. Chung, B.Y. Kang, K.M. Kim, T.S. Kim, Hydroquinone, a reactive metabolite of benzene, enhances interleukin-4 production in CD4⁺ T cells and increases immunoglobulin E levels in antigen-primed mice, *Immunology* 106 (2002) 496–502.
- [33] E. Kim, B.Y. Kang, T.S. Kim, Inhibition of interleukin-12 production in mouse macrophages by hydroquinone, a reactive metabolite of benzene, via suppression of nuclear factor-kappaB binding activity, *Immunol. Lett.* 99 (2005) 24–29.
- [34] Y. Ouyang, N. Virasch, P. Hao, M.T. Aubrey, N. Mukerjee, B.E. Bierer, B.M. Freed, Suppression of human IL-1beta, IL-2, IFN-gamma, and TNF-alpha production by cigarette smoke extracts, *J. Allergy Clin. Immunol.* 106 (2000) 280–287.
- [35] L.A. Geiselhart, T. Christian, F. Minnear, B.M. Freed, The cigarette tar component p-benzoquinone blocks T-lymphocyte activation by inhibiting interleukin-2 production, but not CD25, ICAM-1, or LFA-1 expression, *Toxicol. Appl. Pharmacol.* 143 (1997) 30–36.
- [36] G.B. Post, R. Snyder, Effects of enzyme induction on microsomal benzene metabolism, *J. Toxicol. Environ. Health* 11 (1983) 811–825.
- [37] D.R. Koop, C.L. Laethem, G.G. Schnier, Identification of ethanol-inducible P450 isozyme 3a (P450IIE1) as a benzene and phenol hydroxylase, *Toxicol. Appl. Pharmacol.* 98 (1989) 278–288.
- [38] R. Snyder, T. Chepiga, C.S. Yang, H. Thomas, K. Platt, F. Oesch, Benzene metabolism by reconstituted cytochromes P450 2B1 and 2E1 and its modulation by cytochrome b5, microsomal epoxide hydrolase, and glutathione transferases: evidence for an important role of microsomal epoxide hydrolase in the formation of hydroquinone, *Toxicol. Appl. Pharmacol.* 122 (1993) 172–181.
- [39] S. Kawanishi, S. Inoue, M. Kawanishi, Human DNA damage induced by 1,2,4-benzenetriol, a benzene metabolite, *Cancer Res.* 49 (1989) 164–168.
- [40] L. Zhang, M.L. Robertson, P. Kolachana, A.J. Davison, M.T. Smith, Benzene metabolite, 1,2,4-benzenetriol, induces micronuclei and oxidative DNA damage in human lymphocytes and HL60 cells, *Environ. Mol. Mutagen.* 21 (1993) 339–348.
- [41] A.S. Li, B. Bandy, S. Tsang, A.J. Davison, DNA breakage induced by 1,2,4-benzenetriol: relative contributions of oxygen-derived active species and transition metal ions, *Free Radic. Biol. Med.* 30 (2001) 943–956.
- [42] B. Faiola, E.S. Fuller, V.A. Wong, L. Recio, Gene expression profile in bone marrow and hematopoietic stem cells in mice exposed to inhaled benzene, *Mutat. Res.* 549 (2004) 195–212.
- [43] B.I. Yoon, G.X. Li, K. Kitada, Y. Kawasaki, K. Igarashi, Y. Kodama, T. Inoue, K. Kobayashi, J. Kanno, D.Y. Kim, T. Inoue, Y. Hirabayashi, Mechanisms of benzene-induced hematotoxicity and leukemogenicity: cDNA microarray analyses using mouse bone marrow tissue, *Environ. Health Perspect.* 111 (2003) 1411–1420.
- [44] B. Faiola, E.S. Fuller, V.A. Wong, L. Pluta, D.J. Abernethy, J. Rose, L. Recio, Exposure of hematopoietic stem cells to benzene or 1,4-benzoquinone induces gender-specific gene expression, *Stem Cells* 22 (2004) 750–758.
- [45] E. Noessner, R. Gastpar, V. Milani, A. Brandl, P.J. Hutzler, M.C. Kuppner, M. Roos, E. Kremmer, A. Asea, S.K. Calderwood, R.D. Issels, Tumor-derived heat shock protein 70 peptide complexes are cross-presented by human dendritic cells, *J. Immunol.* 169 (2002) 5424–5432.
- [46] J. Kunisawa, N. Shastri, Hsp90alpha chaperones large C-terminally extended proteolytic intermediates in the MHC class I antigen processing pathway, *Immunity* 24 (2006) 523–534.
- [47] T.R. Sutter, Y.M. Tang, C.L. Hayes, Y.Y. Wo, E.W. Jabs, X. Li, H. Yin, C.W. Cody, W.F. Greenlee, Complete cDNA sequence of a human dioxin-inducible mRNA identifies a new gene subfamily of cytochrome P450 that maps to chromosome 2, *J. Biol. Chem.* 269 (1994) 13092–13099.
- [48] I.A. Pikuleva, I. Bjorkhem, M.R. Waterman, Expression, purification, and enzymatic properties of recombinant human cytochrome P450c27 (CYP27), *Arch. Biochem. Biophys.* 343 (1997) 123–130.
- [49] D. Coletti, E. Yang, G. Marazzi, D. Sassoon, TNFalpha inhibits skeletal myogenesis through a PW1-dependent pathway by recruitment of caspase pathways, *EMBO J.* 21 (2002) 631–642.
- [50] S.E. Boley, V.A. Wong, J.E. French, L. Recio, p53 heterozygosity alters the mRNA expression of p53 target genes in the bone marrow in response to inhaled benzene, *Toxicol. Sci.* 66 (2002) 209–215.